European Rotorcraft Forum

A MULTIBODY MODEL OF THE FLAP STOP CONTACT DYNAMICS OF AN ARTICULATED ROTOR

Giovanni Tovo, giovanni.tovo@leonardocompany.com, Leonardo Helicopters – Yeovil (UK)
Raffaele Frajese, raffaele.frajese@leonardocompany.com, Leonardo Helicopters – Cascina Costa (Italy)

Abstract

The paper discusses a multibody aeroelastic model of an articulated main rotor system. The model is developed with the specific aim to capture the main dynamic features characterising flap stop contact conditions and to provide a means to predict the associated loads. A five bladed fully articulated rotor is considered: blades flexibility is accounted for using beam modal representations and the aerodynamics is modelled with a blade element approach. Particular emphasis is given to the definition of the flap stop mechanism structural and geometrical features, by detailing the contact reaction load paths and importing the contact surfaces from verified 3D CAD geometries. The kinematics of collective and cyclic controls is accurately represented considering servo actuators, rotating and fixed swashplates with the respective scissor links, pitch links and pitch horns. Linear blade lag dampers are implemented reproducing the associated experimental operating damping curve. Special attention is addressed to the model validation activities which lead to the achievement of an encouraging level of correlation with experimental data: the findings highlighted in this paper confirm the validity of the methodology adopted and give confidence in its potential for describing the flap stop contact dynamics of fully articulated rotors.

NOMENCLATURE

AW	AgustaWestland
BB	Beam Bending (positive up)
CB	Chord Bending (positive aft)
FEM	Finite Element Method
LH	Leonardo Helicopter
MPOG	Minimum Pitch On Ground
MR	Main Rotor
TL	Tension Link
D	Contact force damping function
e	Contact force exponent
F_n	Contact force
g	Contact surfaces penetration
$\mu\varepsilon$	TL Fatigue parameter
$\boldsymbol{\theta}$	Control angles vector
$\boldsymbol{S}$	Servo motions vector
$\boldsymbol{T}_S^{\theta}$	Servo motions to control angles transfer function

1. INTRODUCTION

Articulated helicopter rotor systems are usually fitted with mechanical devices aimed at preventing excessive blade flapping excursions. Flap limiters are not designed to engage in flight operating conditions, but contact events have to be considered during ground operations due to a number of possible reasons, such as the combination of particularly severe environmental conditions and aggressive manoeuvres (e.g. windy ship operations).

The change in the blade root conditions induced by a flap stop contact, together with the highly transient dynamic nature of the event, may lead to the rise of abnormal loads in the rotor components affected. Predicting these loads using numerical methods is a challenging task given the complexity of the topic and the variety of disciplines involved, but the implementation of this capability may help investigating the phenomenology, understanding the consequences and preventing the occurrence of such events.

The paper presents a multibody aeroelastic model of an articulated main rotor system developed with the specific aim to capture the main dynamic features characterising flap stop contact conditions and to provide a means to predict the associated loads. A detailed description of the model is reported, emphasising the methodology adopted, the assumptions made and the results obtained: particular attention is given to the model

Presented at 45th European Rotorcraft Forum, Warsaw, Poland, 17-20 September, 2019

validation activities and to the encouraging level of correlation achieved with experimental data.

Section 2 gives a brief overview of the type of events targeted by this activity, and provides a general description of the phenomenology that the model is expected to be able to represent. In section 3 the multibody model is discussed in detail both at system and subsystem level, highlighting the assumptions made at the various stages of the development process. The validation activities are summarized in section 4 where the good level of correlation achieved against flight data is underlined. The conclusions are drawn in section 5.

2. CONTACT EVENTS OVERVIEW

As anticipated above, the objective of this work is to develop a numerical methodology capable of accurately describe and predict the flap stop contact dynamics of fully articulated rotors. The main focus is given to on-ground conditions at nominal MR angular velocity. This is the scenario in which flap stop engagements should be considered, and represents a fairly practical reference to investigate.

During ground operations such as taxiing, rolling take-off or slope landing for instance, the combination of significant cyclic inputs simultaneous to low collective values may lead the MR to experience large amounts of flapping while settled on limited coning angles. Abnormal flapping excursions may also occur when operating in particularly severe environmental conditions: during embarked activities for instance, it is not unusual for the aircraft to encounter strong and gusty winds impinging on the MR at high incidence.

The examples mentioned here above give an idea of the most typical scenarios in which flap stop contact events may be triggered and summarise the kind of conditions addressed by the paper. A limited amount of empirical data available within LH may provide some additional support in better understanding the root cause and the phenomenology associated with such events: Figure 1 and Figure 2 collect some flight test data recorded in the early days of the AW101 helicopter. The two plots describe a flap stop contact incident experienced by the aircraft while manoeuvring on-ground. Figure 1 highlights the characteristic time history of the normalised tension link beam bending moment at a radial station located in proximity of the flap stop mechanism: the 1/rev apart spikes witness a prolonged series of impacts.

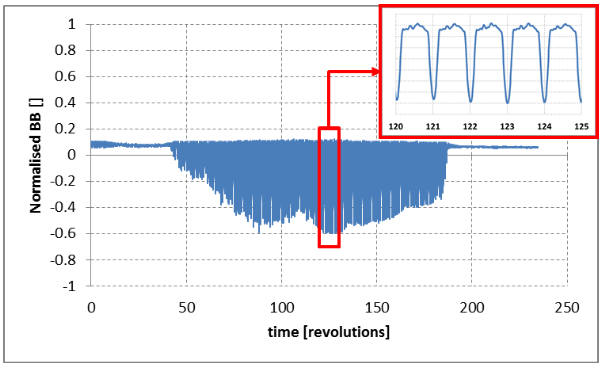

Figure 1: example of MR tension link BB moment time histories during a flap stop contact event

Figure 2 shows the combination of MR controls already described as a potential driver for these events: the collective is dropped near MPOG, and it is interesting to note that the spikes in the BB moment start to develop when the cyclic lever is pulled almost to the aft end of the stroke; the lateral cyclic is maintained in a fairly centred position.

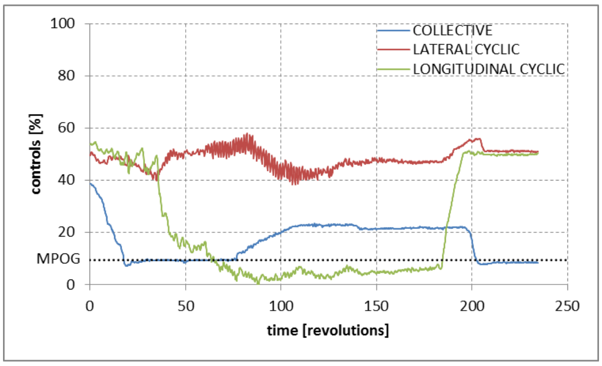

Figure 2: example of MR control time histories leading to a flap stop contact event

It is therefore an essential requirement for the model to be able to reproduce the correct kinematics of main rotor controls and blade motions in order to properly predict flap stop contact onset conditions; in addition to this, only an accurate blade inertial and elastic numerical representation may allow to effectively capture the contact dynamics shown in Figure 1.

3. MULTIBODY MODEL DEVELOPMENT

The various stages followed during the development of the numerical model are detailed in this chapter. After an overview of the overall architecture assembled, each subsystem is described individually in a dedicated section.

Presented at 45th European Rotorcraft Forum, Warsaw, Poland, 17-20 September, 2019

3.1. General description

The multibody model is built using MSC ADAMS[1] and assuming the AW101 fully articulated civil MR system as a reference. Figure 3 and give an idea of the overall representation.

Figure 3: MSC ADAMS model overview

The five blades are modelled using a series of 1D flexible beam elements and introducing the aerodynamic contributions following a blade element approach. Structural and geometrical features of the flap stop mechanisms are finely detailed via an accurate description of contact reaction load paths and contact surfaces. The kinematics of collective and cyclic controls is represented considering servo actuators, rotating and fixed swashplates with the respective scissor links, pitch links and pitch horns. Linear lag dampers are built reproducing the experimental operating damping curve.

3.2. Hub and controls

The control chain circuit is defined in the model thanks to a series of rigid bodies linked together by ideal joints in order to accurately capture the kinematics of the mechanism. Control inputs are applied by prescribing linear motions to the servos, which are connected to ground via three translational joins. Fixed and rotating swashplates transfer these linear motions to the pitch links which allow to control the pitch of the blades through the pitch change arms.

The implemented mechanism is validated using a verified analytical linear kinematic model of the type described by equation (1):

$$(1) \qquad \Delta\boldsymbol{\theta} = \boldsymbol{T}_S^{\theta}\Delta\boldsymbol{S}$$

Where $\Delta\boldsymbol{\theta}$ and $\Delta\boldsymbol{S}$ are vectors describing the variations in control angles and servo displacements respectively; $\boldsymbol{T}_S^{\theta}$ is a linear transfer function. Figure 4 shows some examples of the good match obtained.

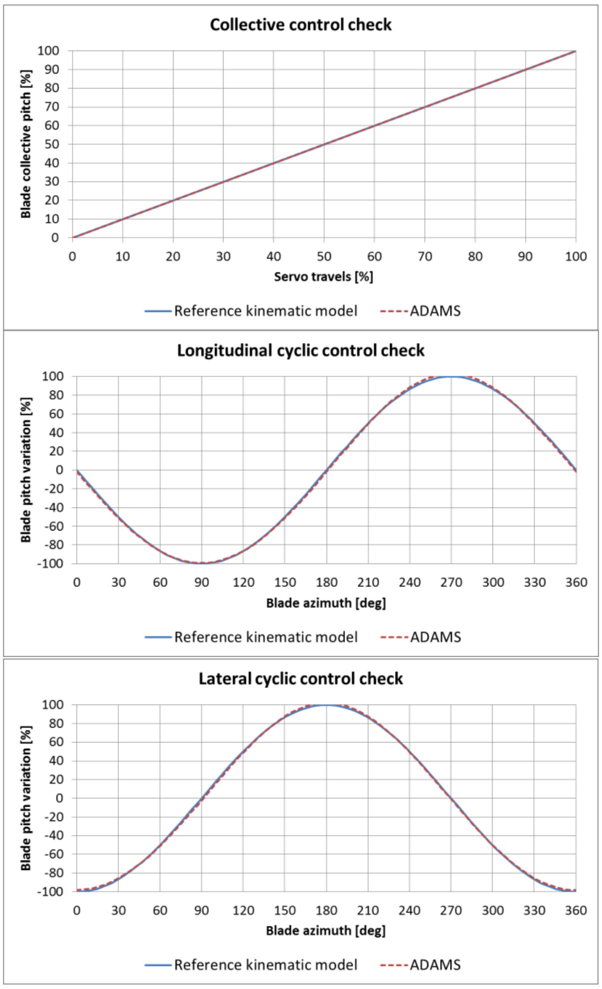

Figure 4: Control chain kinematics validation

The assumption of a rigid control chain is reasonable for the purpose of this paper. In the conditions of interest, described in section 2, the following considerations are found to be valid:

- The flap stop contact dynamics is mainly driven by the blade flapping degrees of freedom.
- The loads on the control chain are not expected to generate relevant elastic deformations on its components.

According to these same arguments, the hub itself is also considered rigid, and is grounded by a rotational joint which may be set to rotate at a prescribed rotor rotational speed. Each lag damper connects a blade to the hub and is modelled as a linear damper implemented according to its characteristic operating curve: see Figure 5.

Presented at 45th European Rotorcraft Forum, Warsaw, Poland, 17-20 September, 2019

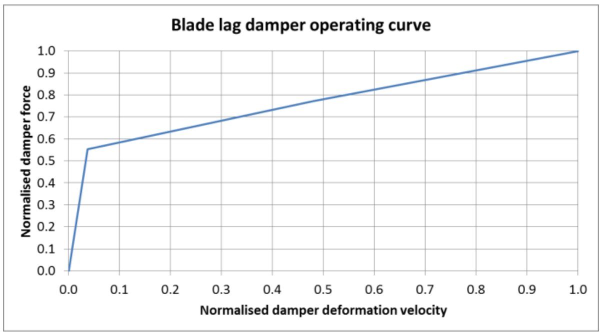

Figure 5: Lag damper operating curve

3.3. MR blade

The MR blade is discretised using one-dimensional structural and aerodynamic elements. A number of flexible bodies, based on FEM beam components and linked together by fixed joints, allow to reproduce the following features:

- The structural dynamic properties (elastic and inertial) of the blade as defined in the available fitting file.
- An appropriate representation of the centrifugal stiffening effect along the blade[2][3].

An additional segmentation is set up to include the aerodynamic properties via several panels defined according to the reference aerodynamic coefficients (C81 tables). The structural elements are built in MSC NASTRAN[4] as CBEAM components and imported in MSC ADAMS using the associated modal description stored in modal neutral file format[4]. The aerodynamic contributions are introduced as a set of concentrated loads distributed along the span; these loads are computed for each panel using a lifting line approach.

Figure 6 summarises the results of a preliminary dynamic validation of the non-rotating free-free blade model performed assuming the legacy LH analytical data as a reference: only the first three flap modes are reported, but a similar level of correlation is also found for lag and torsion modes as well.

A further validation of the blade structural model is performed by setting a cantilever constrain at the root end, and assuming a 1g inertia load. In Figure 7 the BB distribution obtained is compared against both LH legacy predictions and flight test data: the matching is convincing.

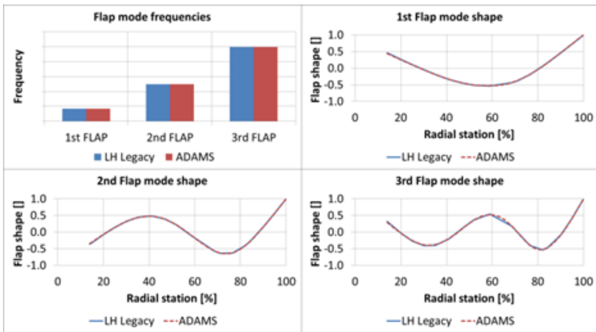

Figure 6: Free-free blade dynamic validation

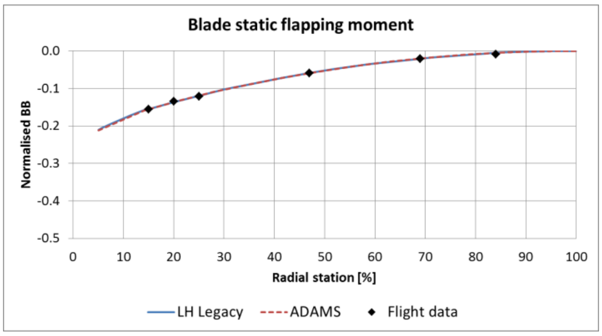

Figure 7: Non rotating blade static validation

The blade model is ultimately verified in terms of aeroelastic predictions. The blade in this case is integrated with the hub and controls sub-system and set to rotate at nominal NR with the collective prescribed to MPOG and cyclic controls centred. Nominal ISA see level conditions with no relative wind are considered. Figure 8 shows the level of correlation achieved between the MSC ADAMS model and the LH legacy results expressed in terms of qualitative blade moment distributions.

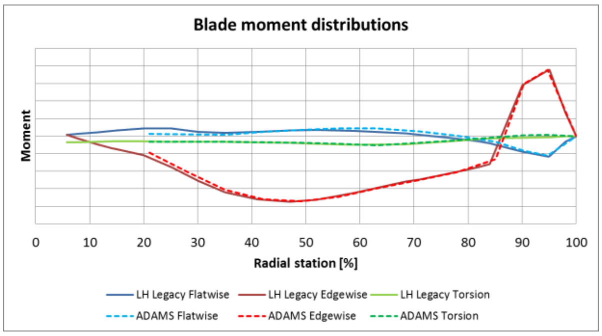

Figure 8: Rotating blade aerodynamic validation

3.4. Tension link model

The modelling of the tension link represents a fundamental step of the activity and requires to be handled with special attention. It is in fact through this component that the flap stop mechanism is implemented and the associated contact reactions are transferred (see section 3.5 for further details on this).

Presented at 45th European Rotorcraft Forum, Warsaw, Poland, 17-20 September, 2019

Figure 9: Tension link overview

Figure 9 and Figure 14 highlight that the modelling strategy adopted for the blade as discussed in section 3.3, is not particularly suitable for the tension link, especially when seeking for describing the flap stop contact dynamics: a single line of beam elements would not be capable of properly capture the contact reactions load path through the inboard portal frame, not to mention the questionable applicability of the beam theory to this component. A fully three-dimensional flexible representation of the tension link would certainly be more appropriate; however this would significantly increase the complexity of the model. A compromise is achievable by using a modelling approach involving multiple lines of beam elements. The idea is summarised in Figure 10: inner and outer portal frames are modelled by means of two lines of beams, representing the upper and lower flange respectively; the anti-torsion wrap in the middle links together the two portals and is assumed to be a single beam line. A number of RBE-like elements are introduced to account for the stiffening effect due to bolted joints, drag limiter, damper attachment and to provide structural connection between flanges and anti-torsion wrap where appropriate. Some non-structural inertia is also distributed on the nodes to include the contribution of lugs, bolts, external fairings etc.

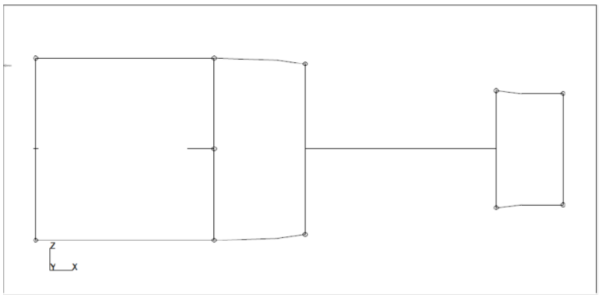

Figure 10: TL MSC ADAMS model

Figure 11, Figure 12 and Figure 13 show the main results of the validation exercise performed on the TL model developed. A verified fully three-dimensional FE model is used as a reference. The static analysis presented in Figure 11 is obtained by setting a cantilever constraint at the blade lugs section of the TL and a prescribed load conveniently applied at the other end; the figure only reports the analysis performed to check the flapping stiffness of the MSC ADAMS model, but the same correlation is confirmed for the stiffness in the other axes as well.

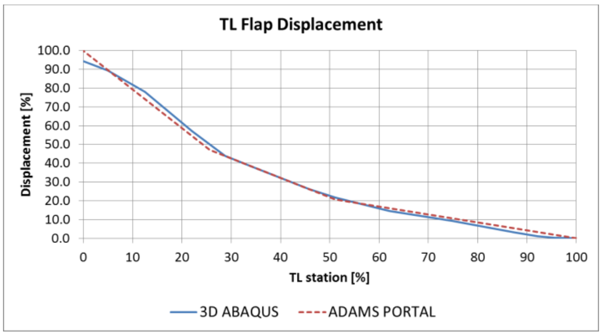

Figure 11: TL model static validation

Figure 12 and Figure 13 report the output of the dynamic validation: only the fundamental flap, lag and torsion mode frequencies and shapes are shown since in the higher frequency modes local phenomena occur and the comparison becomes less meaningful.

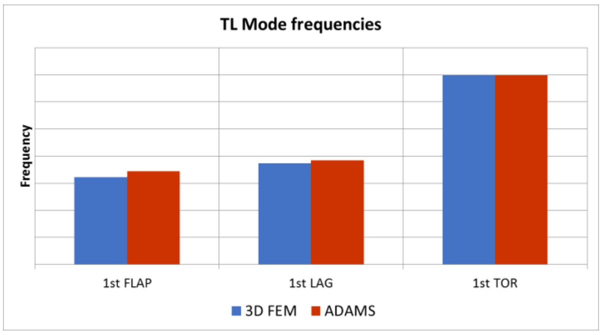

Figure 12: TL dynamic validation – modal frequencies

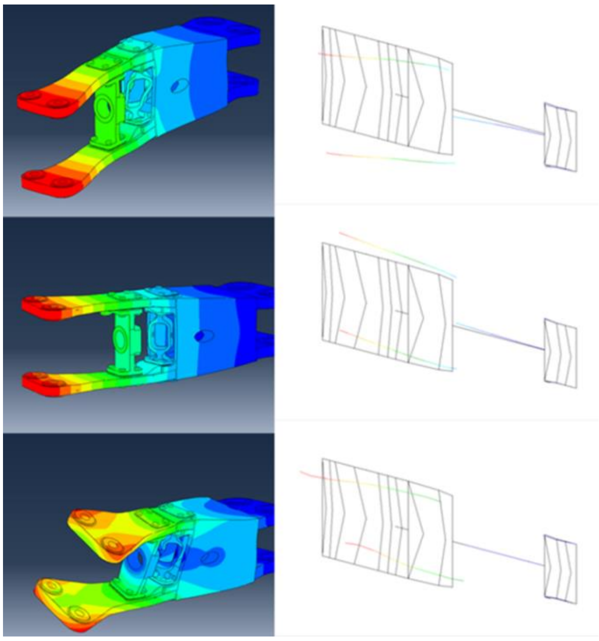

Figure 13: TL dynamic validation – modal shapes

Presented at 45th European Rotorcraft Forum, Warsaw, Poland, 17-20 September, 2019

The findings above are considered acceptable and the TL model validated.

3.5. Flap stop model

The two key components of the AW101 MR flap stop mechanism are the stirrup and the limiter plate (see Figure 14). The former is attached to the hub, the latter is connected to the upper flange of the inner tension link section. Should the blade downward flapping motion reach the allowable limit, a contact between these two surfaces occur and the flap stop is engaged.

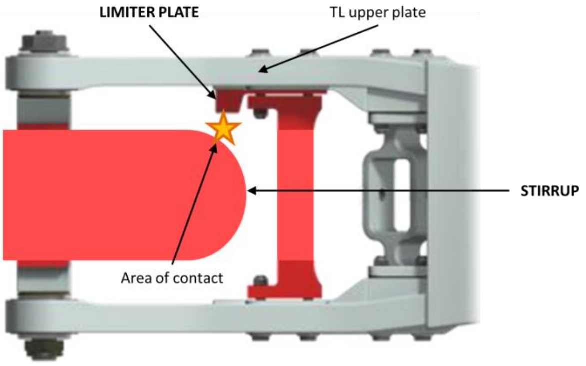

Figure 14: Flap stop mechanism

The flap stop mechanism is represented in the MSC ADAMS model as a contact between two rigid surfaces[1][5] imported from the verified CAD geometries of stirrup and limiter plate respectively. When contact conditions are detected, a reaction is developed between these surfaces. The contact reaction F_n is based on the MSC ADAMS impact force model[1]:

(2) $$F_n = kg^e + D\frac{dg}{dt}$$

Where k is a scalar penalty parameter, g is the penetration between the two geometries, e is a positive real force exponent; D is a damping function that multiplied by the penetration velocity gives a viscous terms that might be used to allow for a more general constitutive relation for the contact bodies and to improve the numerical conditioning of the solution.

The parameters in equation (2) described above are not easy to determine, and are usually dependent upon both contact materials and geometries. This justifies an empirical approach when seeking for their best estimation when dealing with a specific problem: the tuning of these parameters represented the final step of the modelling activity, allowing to successfully correlate the model with the available experimental data as discussed in section 4.

4. MODEL CORRELATION

The multibody model described in the previous section is ultimately correlated against experimental data. As anticipated in section 2, the main difficulty encountered during the correlation exercise is related with the limited amount of flap stop contact evidences recorded in the decades of service of the AW101. The shortage of experimental references was known to be a potential issue for this activity since its kick-off and enforced a significant effort throughout a preliminary feasibility study aimed at recovering flap stop contact occurrences in the LH flight data archives. Only a few instances were found, primarily associated with early flights of some prototype aircraft:

- EVENT #1: Helicopter EHP7CIV, Flight 330, Condition 8, Taxiing on concrete: braking from 30kts to 0 kts.
(March 1994)
- EVENT #2: Helicopter EHP7CIV, Flight 330, Condition 10, 30 kts Run on landing.
(March 1994)
- EVENT #3: Helicopter EHCV510, Flight 110, Condition 2, Taxiing.
(January 1998)

Following these events a set of risk mitigation measures had been taken, and the flap stop contact is no longer considered to be an issue for this helicopter.

These few instances present the same features highlighted in Figure 1 and Figure 2: significant cyclic excursions simultaneous to low collective values, leading to the onset of a well recognisable tension link BB time history pattern. Such pattern is characterised by a sequence of anomalous, one per rev. spikes due to the sudden change in the blade root conditions from hinged to effectively cantilever. The model correlation strategy takes as a main empirical reference a set of strain gauges located both on the TL (just inboard the flap stop radial station) and near the root end of the blade. The multibody simulation is set up running up the rotor to its nominal rotational speed and then conveniently actuating the servos to apply some cyclic sweeps at a prescribed MPOG collective. ISA see level atmospheric conditions are assumed and the effect of the wind is neglected. These settings allow to explore similar conditions to those experienced by the aircraft during the events listed above. Figure 15 to Figure 18 show the correlation obtained between model predictions and flight data.

Figure 15 highlights the effect of a cyclic sweep on a normalized fatigue parameter designated as

Presented at 45th European Rotorcraft Forum, Warsaw, Poland, 17-20 September, 2019

με: this parameter is defined as a linear combination of beam and chord bending moments acting on a TL section just inboard the flap stop device.

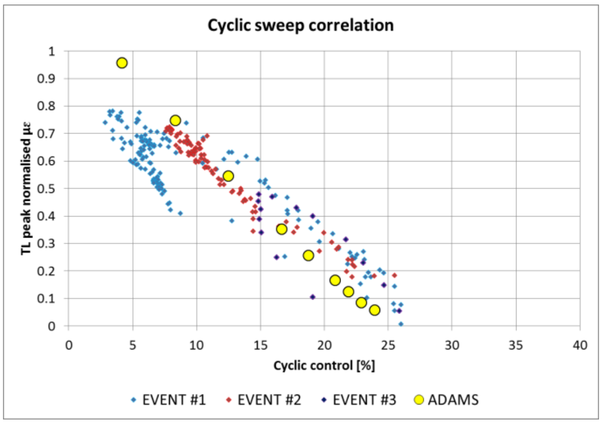

Figure 15: Cyclic sweep correlation

The three clouds of dots and the yellow circles represent respectively empirical and predicted peak values of με expected when flap stop contact conditions occur. It is quite encouraging to note that flight data are quite repeatable and the model is reasonably capable of capturing the expected amount of cyclic at which the flap stop engages: at lower cyclic values the blade flapping excursions are not sufficiently high to trigger the stop, and the με remains close to zero. It is also interesting to highlight that the empirical ratio between contact severity and cyclic variation is well matched by the model predictions. The slight mismatch in the position of the intercept seems consistent with the level of approximation accepted for the model, considering in particular that no attempt is made to include ground effect or fuselage upwash in the aerodynamic representation. To further reinforce the validity of the correlation achieved, it should be considered that a minor model correlation correction applied to the cyclic input would be sufficient to shift the predicted dataset allowing it to fully envelope the flight data in Figure 15: such a correction would need to be of the same order of the uncertainties affecting the control circuit instrumentation measurements.

Figure 16, Figure 17 and Figure 18 collect some time history correlations obtained focusing around the 5% cyclic control input snapshot of Figure 15. Beam bending moment and chord bending moment at the flap stop section of the tension link, and blade beam bending moment near the blade root are reported. The three plots confirm the effectiveness of the model in predicting not only the peak contact loads, but also the main dynamic content of the response of the rotor system components primarily involved in flap stop contact events. The minor mismatch primarily affecting the BB time histories does not seem to indicate any gross inaccuracies impacting the model.

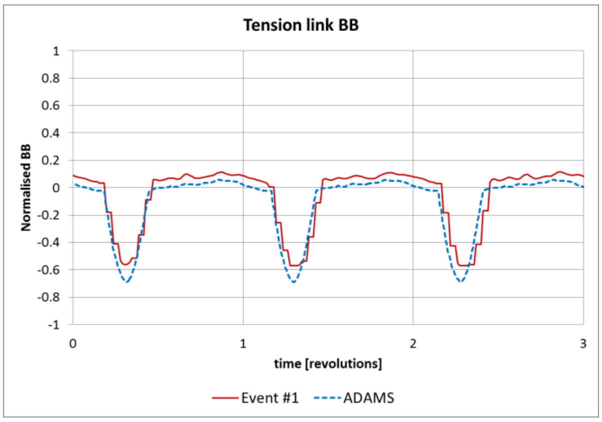

Figure 16: TL BB time history correlation

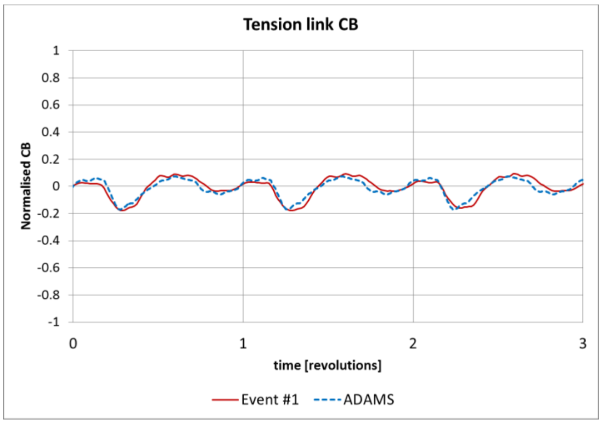

Figure 17: TL CB time history correlation

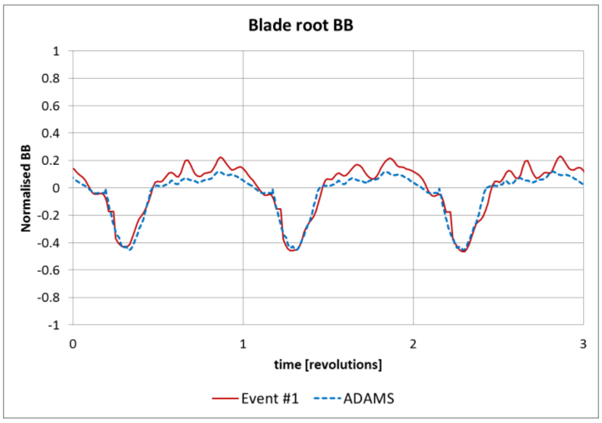

Figure 18: Blade BB time history correlation

The results presented here above are considered satisfactory and the MR model is proven to be adequately representative of the physical system.

5. CONCLUSION

A MSC ADAMS multibody aeroelastic model of a fully articulated main rotor system is presented in this work. The emphasis is addressed to the detailed numerical representation of the elements through which the flap stop mechanism is implemented. The model developed is confirmed to successfully meet the objective of this activity, demonstrating the potential of the methodology adopted to accurately describe the flap stop contact dynamics of articulated rotor systems.

An interesting finding to be highlighted is that, for the purpose of this research, the dynamic of a complicated three-dimensional structure such as the main rotor tension link might be adequately modelled using a convenient frame of one-dimensional beam elements: this approach is certainly preferable to a fully 3D FE representation, allowing for instance to save computational resources and to easily interrogate the model.

Even though the level of correlation achieved with flight data is considered satisfactory, it is worth mentioning that the assumptions accepted during the modelling exercise may be relaxed, i.e.: control chain flexibility, 3D FE representation of the tension link, higher order aerodynamic terms and so on could certainly be considered as future developments.

6. REFERENCES

[1] MSC Software Corporation – ADAMS Documentation

[2] Jose L. Ortiz, Gunjit S. Bir: "*Verification of New MSC.ADAMS Linearization Capability For Wind Turbine Applications*", 44th AIAA Aerospace Sciences Meeting and Exhibit, 9-12 January 2006, Reno, Nevada.

[3] Jose L. Ortiz, Gunjit S. Bir: "*A Practical Approach for the Linearization of the Constrained Multibody Dynamics Equations*", 2006

[4] MSC Software Corporation – NASTRAN Documentation

[5] C. L. Bottasso et al.: "*Unilateral Contact Modelling with ADAMS*"

Presented at 45th European Rotorcraft Forum, Warsaw, Poland, 17-20 September, 2019